

Sulfonic-functionalized Graphene Quantum Dots as a Highly Efficient Fluorescent Probe for Fe(III) Ions Detection

DOI: 10.25177/JCCMM.2.3.1

Research

Received Date: 28th Apr 2018Accepted Date: 27th Jun 2018Published Date: 08th Jul 2018

Copy rights: © This is an Open access article distributed under the terms of International License.



Chenjie Yao,^{a+} Xiaojun Xing,^{a+} Wenchao Gao,^a Lin Ding,^a Peng Dong,^a Chenchen Li,^a Yanan Huang,^a Minghong Wu,^{b*} Yanli Wang^{a*}

^aInstitute of Nano-chemistry and Nano-biology, Shanghai University, Shanghai 200444, P.R. China

^bSchool of Environmental and Chemical Engineering, Shanghai University, Shanghai 200444, P.R. China

⁺These authors contribute equally to the paper.

CORRESPONDENCE AUTHOR

Prof. Ming Hong Wu, School of Environmental and Chemical Engineering, Shanghai University, Shanghai 200444, P.R. China. E-mail: mhwu@shu.edu.cn

Prof. Yan Li Wang, Institute of Nano-chemistry and Nano-biology, Shanghai University, Shanghai 200444, P.R. China. E-mail: wangyanli@staff.shu.edu.cn

CONFLICTS OF INTEREST

There are no conflicts of interest for any of the authors.

CITATION

Yanli Wang, Sulfonic-functionalized Graphene Quantum Dots as a Highly Efficient Fluorescent Probe for Fe(III) Ions Detection (2018) SDRP Journal of Computational Chemistry & Molecular Modelling 2(3) p:179-189

ABSTRACT

Background:

Graphene quantum dots (GQDs), a novel type of graphene nanomaterial, have attracted tremendous attention. Much better performance of application of functionalize GQDs in ions detection have been proved.

Here, we propose a rapid and facile strategy to detect Fe³⁺ ions by sulfonic graphene quantum dots (sulfonic-GQDs).

Methods:

The sulfonic-GQDs were synthesized by a modified hydrothermal molecular fusion method. The procedures for detection of Fe³⁺ ions were described con-

cretely in the main text, and the fluorescence quenching principle was also performed. Results were expressed as mean ± standard deviation (SD).

Results:

It was observed that the Fe³⁺ ions could efficiently quench the fluorescence of sulfonic-GQDs. With the optimized conditions, the sulfonic-GQDs exhibit high sensitivity and selectivity for fluorescence probe to detect the Fe³⁺ ions with the calibration curve displays linear regions over the range of 5-100 μM and a detection limit of 407 nM. In addition, sulfonic-GQDs fluorescent probe show very good selectivity of the Fe³⁺ ions detection. There is no obvious interference with detect of Fe³⁺ ions when in the simulated complex sys-

tem with the existence of the other common metal ions. The possible fluorescence quenching mechanism between Fe^{3+} ions and sulfonic-GQDs were discussed. The experimental results indicate that the interaction between Fe^{3+} ions and sulfonic-GQDs is dominated by static quenching process.

Conclusion:

The sulfonic-GQDs with high chemical and photo stability are in a very good biocompatibility which shows great promising applications in the environment water sample analysis, food analysis and clinical diagnosis.

Key words: Fe^{3+} ions, Sulfonic-GQDs, Detection, Fluorescence quenching mechanism

1. INTRODUCTION

Fe^{3+} ions is an essential trace element in biological system[1] and food products[2]. Moreover, as industrial and other anthropogenic processes, heavy metal ion pollution has been constantly valued because of severe risks in human health and the environment evolution in recent years[3]. It plays a crucial role in many biological processes because of its wide existence in electron transport, oxygen transport and as a catalyst in oxido-reductase reactions[4, 5]. Both deficiency and excess can cause biological toxicity, such as cellular homeostasis and metabolism[6, 7]. Fe^{3+} ions has been connected with serious diseases, including Huntington's, Parkinson's and Alzheimer's disease[7].

At present, several analytical techniques have been used for determination of trace amounts of Fe^{3+} ions, such as voltammetry[8], spectrophotometry[9-11], atomic absorption spectrometry[12], and inductively coupled plasma mass spectrometry (ICP-MS) [13], etc. However, these instrumental techniques require sophisticated instrumentation and tedious sample preparation procedures, which limit the practical applications in routine Fe^{3+} ions detection. Recently, the fluorescent Fe^{3+} ions sensors have become particularly attractive due to their high sensitivity, great simplicity, easy monitoring, and rapid response, providing a better choice for the detection of Fe^{3+} ions. The sensors can bind to Fe^{3+} ions and form various composites, and thus changes the fluorescence values[14, 15]. Several

reported[16-21] fluorescence (FL) probes are poisonous, biologically incompatible, and water-insoluble, which greatly limited the application of detection of Fe^{3+} ions. Therefore, new novel FL probes with easy preparation procedure, low cytotoxicity, high water solubility, high sensitivity and selectivity for Fe^{3+} ions measurement is of vital importance.

Graphene quantum dots (GQDs), a novel type of graphene nanomaterial, have attracted tremendous attention because of their chemical inertness, high and stable photoluminescence (PL), good dispersibility in water, tunable surface functionalization, excellent biocompatibility and environmentally-friendly characteristics [22-24]. On the basis of these unique properties, various GQDs-based fluorescent probes have emerged as potential candidates to be applied in biological application and chemical analysis[23-28]. Much better performance of application of functionalize GQDs in ions detection have been proved[22, 23, 29, 30]. Several successful examples have been reported to determine some ions, such as Eu^{3+} [31], Hg^{2+} [32], Cu^{2+} [33], Fe^{3+} [3, 14, 15] and Cl^- [34] by FL intensity changes of functionalized GQDs. Rhodamine-functionalized graphene quantum dots were used to detect Fe^{3+} ions in cancer stem cells with the detection limits as low as $0.02 \mu\text{M}$ [15]. Nitrogen-doped graphene quantum dots fluorescence probe shows a sensitive response to Fe^{3+} ions in a wide concentration range of $1\text{-}1945 \mu\text{M}$ with a detection limit of 90 nM [14]. However, cost-effective, time-efficient, and process-simple methods for the preparation of GQDs for selective sensing are still urgently needed[3]. In this paper, we present a simple, economical, and green method for detection of Fe^{3+} ions based on sulfonic-functionalized graphene quantum dots (sulfonic-GQDs) by a hydrothermal molecular fusion method [22] and it can be easily mass produced. The sulfonic-GQDs exhibited sufficient water solubility and excellent FL properties. Meanwhile, a label-free sensing platform based on the as-prepared sulfonic-GQDs have been developed and showed a sensitive response to Fe^{3+} ions in the concentration range of $5\text{-}100 \mu\text{M}$ with a detection limit of 407 nM . The results indicate that the detection system with the sulfonic-GQDs- Fe^{3+} have good selectivity in the simulated complex system

of environment which show a hopeful future for the application of sulfonic-GQDs as sensing platform in environmental systems and other biological samples. Furthermore, the FL quenching mechanism was studied by the UV-vis absorbance analysis, and time correlated single photon counting (TCSPC) experiments. Based on the results we deduce that the quenching mechanism of the sulfonic-GQDs-Fe³⁺ ions detection system is to be predominantly by the static rather than dynamic type.

2. MATERIALS AND METHODS

2.1. Materials and Reagents

All reagents used in this work are analytical reagent grade and commercially available. Pyrene, sodium sulfite, tris(hydroxymethyl)aminomethane, nitric acid and hydrochloric acid was purchased from Sinopharm Chemical Reagent Co. Ltd. Solutions of Fe³⁺, K⁺, Ca²⁺, Na⁺, Mg²⁺, Zn²⁺, Cu²⁺, Co²⁺, Mn²⁺ ions were prepared from their chloride salts. And all aqueous solutions were prepared with distilled water produced by a Milli-Q system (R > 18.1 MΩ cm).

2.2. Instrumentation

The morphology and structure of sulfonic-GQDs were investigated using high resolution transmission electron microscopy (HRTEM, JEM-2010F, Japan) and transmission electron microscopy (TEM, JEM-200CX, JEOL, Japan). The size distribution of sulfonic-GQDs were computed using software (ImageJ) based on the size information of more than 400 particles in the images. All steady state UV/Vis absorption and FL spectra measurements were carried out with a Hitachi 3100 spectrophotometer (Tokyo, Japan) and Hitachi F-7000 FL spectrophotometer (Tokyo, Japan) using a 1 cm path length quartz cell at room temperature. The Fourier transform infrared spectroscopy (FT-IR) spectrum was performed on an AVATAR 370(Nicolet, USA) spectrometer. The hydrate particle sizes of Fe³⁺, sulfonic-GQDs and sulfonic-GQDs+Fe³⁺ composite were measured on a Nanosizer (Zetasizer 3000 HS, Malvern, UK).

2.3. Synthesis of sulfonic-GQDs

The sulfonic-GQDs were synthesized by a modified hydrothermal molecular fusion method established by us[22]. Briefly, pyrene (1g, TCI, purity 98%) was nitrated into 1, 3, 6- trinitropyrene in hot HNO₃ (50 ml) at 80 °C under reflux with vigorous stirring for 24 h. After cooled to room temperature, the mixture was diluted with deionized (DI) water and filtered through a 0.22 μm microporous membrane (TOPTION, M50-22-F Microporous Membrane) to remove the redundant acid. The resultant yellow 1, 3, 6- trinitropyrene was dispersed in an Na₂SO₃ solution of DI water (100ml, 0.5 M) under stirring for 0.5 h. The suspension was transferred to a poly (tetrafluoroethylene) lined autoclave and heated at 200 °C for 12 h. After being cooled to room temperature, the product containing water-soluble sulfonic-GQDs was dialyzed in a dialysis bag (retained molecular weight: 3,500 Da) for 2 days to remove sodium salt and unfused small molecules and dried at 80 °C for quantification.

The QY of the as-synthesized sulfonic-GQDs was calculated by measuring the fluorescence intensity in aqueous dispersion based on quinine sulfate as a standard following equation:

$$\Phi_x = \Phi_{qs} \frac{I_x}{I_{qs}} \frac{\eta_x^2}{\eta_{qs}^2} \frac{A_{st}}{A_x}$$

where Q is the quantum yield, I is the measured intensity of luminescent spectra, A is the optical density at excitation wavelength and the subscript “qs” refers to the standard with a known quantum yield QY using quinine sulfate in 0.05 M sulfuric acid solution (literature QY 0.54 at 310 nm), and “x” refers to the sample. In order to minimize reabsorption effects, absorbance in the 10 mm fluorescence ---cuvette were kept under 0.05 at the excitation wavelength (365 nm).

2.4. Procedures for detection of Fe³⁺ ions

Stock standard solutions 10 mM Fe³⁺ was prepared by dissolving an appropriate amount of FeCl₃·6H₂O in Tris-HCl (20 mM, pH = 7.0) buffer solution adjusting the volume to 10.0 mL in a volumetric flask at room

temperature. It was further diluted to 1×10^{-3} to 1×10^{-5} M stepwise. In a typical run, 2 mL Tris-HCl buffer solution of sulfonic-GQDs ($20 \text{ mg}\cdot\text{mL}^{-1}$) was added in a centrifuge tube (5 mL) and then 2 mL various concentrations of Fe^{3+} ions were added. The solution was mixed thoroughly by a vortex generator and incubated at room temperature for 10 min before FL spectral measurements. All the FL detections were conducted under the same conditions and the emission wavelength was recorded within the range of 380–650 nm with a fixed excitation wavelength of 368 nm. The interfering effects of other metal ions and food additives were investigated individually.

2.5. Fluorescence quenching principle

All FL spectra were recorded on the F-7000 spectrophotometer by fitting the excitation wavelengths at 368 nm with thermostatic water bath. The reported FL quenching mechanism usually includes collisional process (dynamic quenching) and/or ground state complex formation (static quenching) between quencher and fluorophore that can be easily distinguished by lifetime measurements. Since the life-time of the fluorophore is unperturbed by the static quenching, when it is $\tau_0/\tau = 1$, τ_0 and τ are the lifetime of the fluorophore in the absence and presence of the quenchers, respectively.

2.6. Cell cytotoxicity assay

The cytotoxicity of sulfonic-GQDs towards GES-1 cells was evaluated by the CCK-8 method. The GES-1 cells were seeded into 96 wells culture plate and then incubated overnight in an incubator. After the culture medium was removed, GQDs with different concentrations were added into each well. Cells were then allowed to incubate for another 24 h. Then, CCK-8 (10 ml per well) solution was added in each well and incubated at 37°C for 1 h. The absorbance was measured at 450 nm by the Enzyme standard instrument.

2.7. Statistical analysis

Results were expressed as mean \pm standard deviation (SD). Comparisons among the groups were evaluated by *t*-test or ANOVA followed by the Student-Newman

-Keuls test. A value of $p < 0.05$ was considered statistically significant.

3. RESULTS AND DISCUSSION

3.1. Characterizations

The morphology and structure of the as-prepared sulfonic-GQDs under the hydrothermal molecular fusion synthesis conditions were investigated by TEM and HRTEM. Figure 1a shows the TEM images of the GQDs dispersed in water. As displayed from the TEM image, their diameters were mainly distributed in the narrow range of 2–4 nm with an average size of 2.8 nm (Figure 1b), suggesting that the as-prepared sulfonic-GQDs were uniformly arranged. The high resolution HRTEM image (inset of Figure 1a) indicates the sulfonic-GQDs are almost defect-free graphene single crystals with a spacing of 0.22 nm corresponding to that of graphene planes[35].

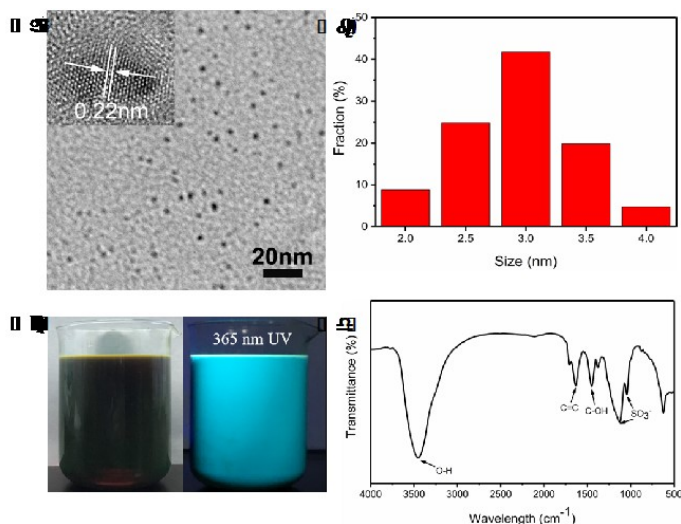


Figure 1. (a) TEM image of the as-prepared sulfonic-GQDs, Scale bar: 20 nm, the inset is the HRTEM image. (b) Size distribution of sulfonic-GQDs. (c) Photographs of aqueous colloids of sulfonic-GQDs be synthesized by mass production. (d) The FT-IR spectra of sulfonic-GQDs.

The synthesis systems of sulfonic-GQDs can be mass produced with high quantum yield (QY). Figure 1c shows that the picture of aqueous colloids of sulfonic-GQDs under sunlight and a 365 nm UV lamp. The QY of GQDs was measured to be 45.7%, rendering them highly sensitive fluorescent probes (<15% in

most cases[36, 37]). The functional groups on the surface of the as-prepared sulfonic-GQDs were identified by FT-IR spectroscopy. Figure 1d shows that the absorption of asymmetric and symmetric stretching vibration of SO₃ at 1128 and 1045 cm⁻¹, C=C at 1633 cm⁻¹, C-OH at 1376 cm⁻¹ and O-H at 3454 cm⁻¹. The results of FT-IR indicate that the sulfonic-GQDs are rich in sulfonic and hydroxyl groups on their surfaces. These functional groups improved the hydrophilicity and stability of the sulfonic-GQDs in an aqueous system.

The results of UV-vis absorption and PL emission spectra of sulfonic-GQDs dispersed in aqueous solution are shown in Figure 2a. A typical UV-Vis spectrum exhibited three pronounced excitonic absorp-

tion bands at ca. 244, 290 and 374 nm which were assigned to the π - π^* transition of aromatic C=C sp² domains[3, 38]. Moreover, sulfonic-GQDs had the maximum FL emission (Em) wavelengths at 472 nm on the excitation of 368 nm, and the FL excitation (Ex) spectrum shows peak at 296 and 379 nm with the corresponding excitonic absorption bands, suggesting that the emission is characterized by band edge exciton-state decay rather than defect-state decay[35]. As shown in the inset of Figure 2a, a blue-green luminescence of sulfonic-GQDs solution were irradiated by a 365 nm UV lamp. The emission peak of sulfonic-GQDs was shifted to longer wavelengths with the excitation wavelength changed from 350 to 460 nm which means sulfonic-GQDs exhibit an excitation-dependent luminescent behavior (Figure 2b)[39].

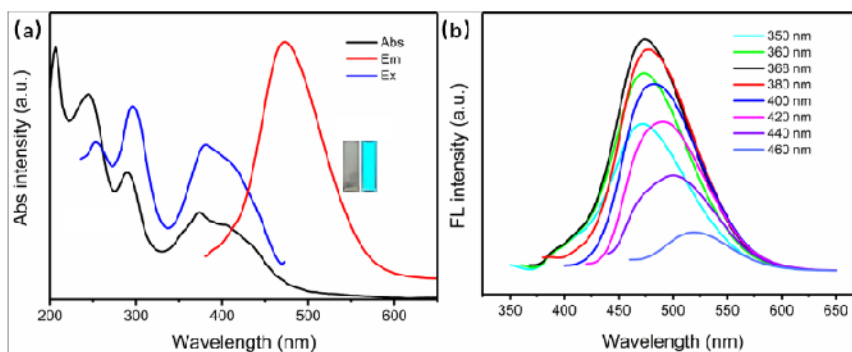


Figure 2. (a) UV-vis absorption, FL emission (Em) and excitation (Ex) spectra of sulfonic-GQDs. The inset shows the photographs of aqueous dispersions of sulfonic-GQDs under day light (left) and UV (365 nm) illumination (right). (b) PL spectra of 20 mg·mL⁻¹ sulfonic-GQD solution under different excitation wavelength.

3.2. Optimization of sensing conditions

In order to obtain the best performance for Fe³⁺ ions assay, the following optimization experiments were performed to gain the most appropriate conditions.

3.2.1. Optimal reaction temperature and time

The most optimal reaction temperature and time were selected by exploring the FL stability of sulfonic-GQDs before and after adding the Fe³⁺ ions under a Xe lamp at different temperatures and times. As shown in Figure 3a, the degree of quenching decreased as the temperature increased. The linear relationship between fluorescence and quencher was best

at 25 °C after further temperature-change study, while 25 °C was considered to be the best temperature for Fe³⁺ detection (Figure 3c and Table. 1). In addition, we studied the dynamics of the reaction at 25 °C to optimize the reaction time for detection of Fe³⁺ ions, as shown in Figure 3b. At this temperature, the quenching process was completed in under 10 min. This level of quenching was maintained for 60 min and no loss of fluorescence was observed in the control sample. This result shows that sulfonic-GQDs had excellent photostability. In sum, 25 °C and 10 min were selected as the optimal reaction temperature and reaction time for sulfonic-GQDs and Fe³⁺ ions, respectively.

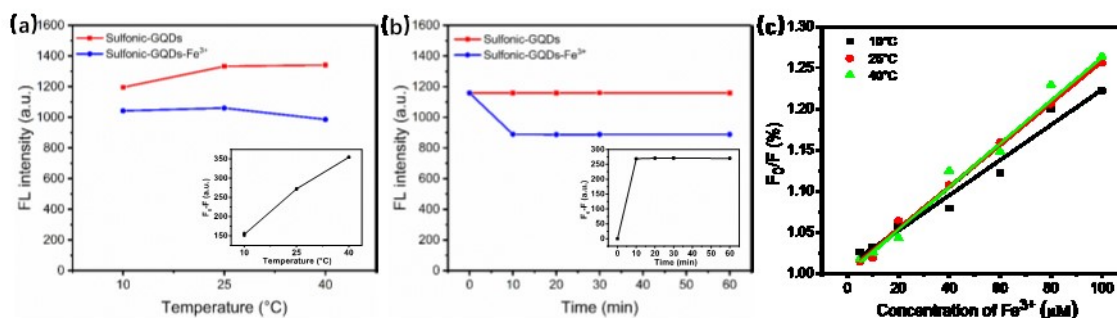


Figure 3. Optimization sensing conditions of temperature and time. (a) FL intensity of sulfonic-GQDs and sulfonic-GQDs with Fe³⁺ at different temperatures. Insert: The curve of the fluorescence quenching values F_0/F vs Fe³⁺ at various temperature. F_0 and F represent the FL intensities of sulfonic-GQDs at 472 nm in the absence and presence of Fe³⁺ ions, respectively. (b) Photostability measurement of sulfonic-GQDs and sulfonic-GQDs with Fe³⁺ at different time points. Insert: The curve of the fluorescence quenching values F_0/F vs Fe³⁺ at various time points. F_0 and F represent the FL intensities of sulfonic-GQDs at 472 nm in the absence and presence of Fe³⁺ ions, respectively. (c) The plots of Stern–Volmer equation at three different temperatures.

Table 1. Sulfonic-GQDs detection Fe³⁺ under the three temperatures, correlation coefficient R^2 .

System	T (°C)	The equation for linear regression	R^2
Sulfonic-GQDs-Fe ³⁺	10	$F_0/F=1.0093+0.0021C$	0.9875
	25	$F_0/F=1.0033+0.0025C$	0.9994
	40	$F_0/F=1.0005+0.0026C$	0.9871

3.2.2. Effect of pH and buffer

In order to achieve the best performance for Fe³⁺ ions assay, different pH values and reacting buffers were studied and optimized. Figure 4a shows that varying pH values from 7.0 to 9.0 had little effect on the initial FL intensity of sulfonic-GQDs, while distinct changes occurred in the system of sulfonic-GQDs with Fe³⁺ ions. This result indicated that the control of pH value

plays crucial role in Fe³⁺ ions detection and had great quenching effect in neutral media than others. Obviously, as show in Figure 4b, the quenching efficiency of sulfonic-GQDs under different reacting buffer (Tris-HCl buffer, PBS buffer and HEPES buffer) was quite different. The highest quenching efficiency was detected in Tris-HCl buffer (20 mM, pH=7.0), suggesting that Tric-HCl buffer was the most suitable for the proposed strategy.

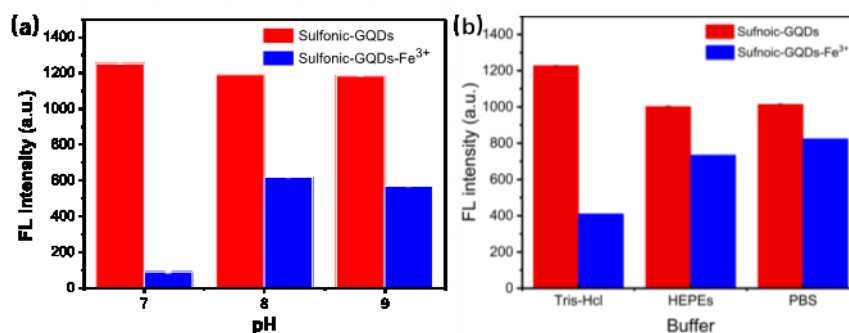
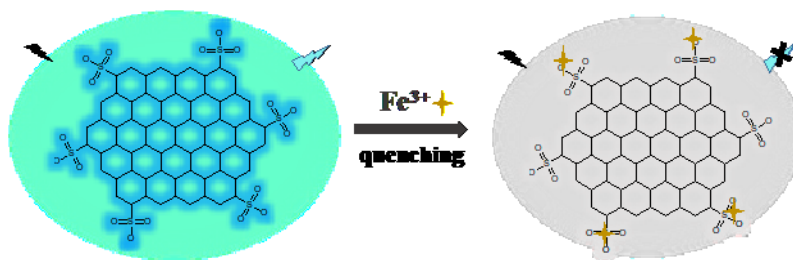


Figure 4. Optimization sensing conditions of (a) FL intensity of sulfonic-GQDs and sulfonic-GQDs with Fe³⁺ under different pH values, (b) FL intensity of Sulfonic-GQDs and sulfonic-GQDs with Fe³⁺ under in three types of buffer.

3.3. Sensitivity and selectivity study of Fe^{3+} ions detection



Scheme 1. Fluorescence quenching mechanism of the sulfonic-GQDs in the presence of Fe^{3+} ions.

The previous studies[38, 40] indicated that use of GQDs or carbon dots to detect Fe^{3+} based on the specific coordination between chemical group and Fe^{3+} ions. Given the special covalent binding between Fe^{3+} ions and sulfonic, exploration was begun into the feasibility of the sulfonic-GQDs FL response to Fe^{3+} ions. The proposed detection system can coordinate with chemical groups on the edge of sulfonic-GQDs with Fe^{3+} and induce the FL intensity change (Scheme.1). All FL detection experiments were conducted under the optimal conditions and the emission wavelength was recorded within the range of 380-650 nm with a fixed excitation wavelength of 368 nm. We show the sensitivity of sulfonic-GQDs fluorescent probes for the detection of Fe^{3+} ions. As shown in Fig-

ure 5a, it was found that the intensity of the FL at 472 nm decreased gradually with increasing concentrations of Fe^{3+} ions ranged from 0 to 1000 μM and the emission was quenched completely by Fe^{3+} ions at the high concentration of 1000 μM . Accordingly, the color of sulfonic-GQDs changed from bright blue-green to weak blue-green under UV irradiation (the inset of Figure 5a). Figure 5b indicates that FL quenching value ΔF ($F_0 - F$) with the concentration of Fe^{3+} ions in the range of 5 ~ 100 μM has a good linear relationship. The equation for linear regression is $\Delta F = 2.996C + 10.111$ with a correlation coefficient of 0.9927, where C is the concentration of Fe^{3+} ions (μM). The detection limit was estimated to be 407 nM (according to a signal-to-noise ratio of 3).

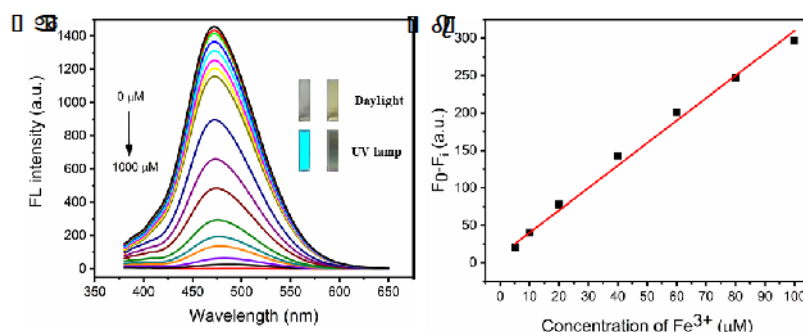


Figure 5. (a) Fluorescence spectra of sulfonic-GQDs with different concentrations of Fe^{3+} (from top to bottom: 0, 5, 10, 20, 40, 60, 80, 100, 200, 400, 500, 600, 700, 800, 900, 1000 μM , respectively); inset: the photographs of the fluorescence response of sulfonic-GQDs upon addition of Fe^{3+} at 0 and 1000 μM under daylight (up) and UV lamp (down). (b) The curve of the fluorescence quenching values ΔF vs Fe^{3+} concentration ranging from 0 to 100 μM . $\Delta F = F_0 - F$, F_0 and F represent the FL intensities of sulfonic-GQDs at 472 nm in the absence and presence of Fe^{3+} ions, respectively.

In order to assess the selectivity of the method, the selectivity of our sulfonic-GQDs was investigated. We assessed quenching of sulfonic-GQDs upon exposure to 500 μM Fe^{3+} , K^+ , Ca^{2+} , Na^+ , Mg^{2+} , Zn^{2+} , Cu^{2+} , Co^{2+} , Mn^{2+} . Figure 6 shows the FL intensity ratios (F/F_0) of sulfonic-GQDs solution in the absence and presence of various metal ions. None of these ions affected FL. In addition, a cocktail of all these ions (100 μM each; including Fe^{3+}) showed similar quenching to what was observed with Fe^{3+} alone, indicating that there are no compensating effects. Furthermore, the mass production, good chemical and photo-stability of sulfonic-GQDs, which show the great potential of sulfonic-GQDs probe for the potential to in real environment and food samples detection.

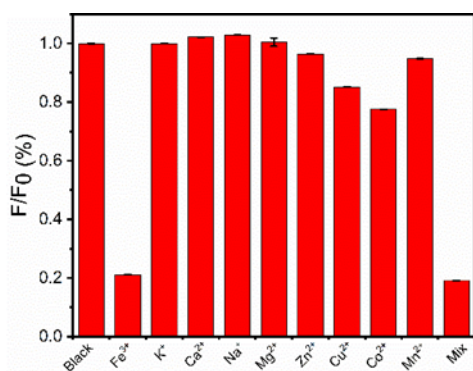


Figure 6. Fluorescence intensity ratios (F/F_0) of sulfonic-GQDs in the presence and absence of different metal ions (500 μM). listed from left to right: Blank, Fe^{3+} , K^+ , Ca^{2+} , Na^+ , Mg^{2+} , Zn^{2+} , Ti^{2+} , Cu^{2+} , Co^{2+} , Mn^{2+} and mixed. The mixed solution contains all of the metal ions mentioned above. The error bars represent the standard deviations based on the independent measurements.

3.4. Mechanism of the Fluorescence quenching

To further study the quenching mechanism of sulfonic-GQDs by Fe^{3+} , time-correlated single-photon counting (TCSPC) experiments were used to test the charge transfer and exciton recombination process of sulfonic-GQDs in the presence and absence of Fe^{3+} ions[41]. In the presence of Fe^{3+} ions, the lifetime of sulfonic-GQDs fluorescence shifted slightly from 4.70 ns to 4.74 ns (Figure 7a). The FT-IR spectra in Figure 7c further showed that new absorption peaks appeared after Fe^{3+} was mixed with sulfonic-GQDs which mean

new chemical reactions occurred, and was attributed to electrostatic interaction and π - π stacking interaction. We, thus, deduced that in this case, the quenching mechanism of sulfonic-GQDs for Fe^{3+} detection involves complexation (static quenching) rather than collisional deactivation (dynamic quenching).

The UV-vis absorption spectra of sulfonic-GQDs in the absence and presence of Fe^{3+} ions in solution are shown in Figure 7b. The UV-vis absorption spectrum of sulfonic-GQDs shows an absorption band at ca. 240 and 290 nm. However, it is well-known that an absorbance vanished were observed upon the addition of Fe^{3+} ions. Furthermore, the morphology of composites was observed by TEM (Figure 7d) which was found that sulfonic-GQDs and Fe^{3+} ions could accumulate together and form the composite agglomeration. In Table. 2, we also detected the hydrate particle sizes of Fe^{3+} , sulfonic-GQDs and sulfonic-GQDs+ Fe^{3+} composite, which indicated that the size of composite increased a lot comparing to Fe^{3+} ions or GQDs (the hydrate particle size of GQDs could not be detected by DLS), confirming the aggregation of the composite. The results should be attributed to the combination of Fe^{3+} ions with sulfonic-GQDs, suggests that the quenching process by Fe^{3+} ions is static quenching[38].

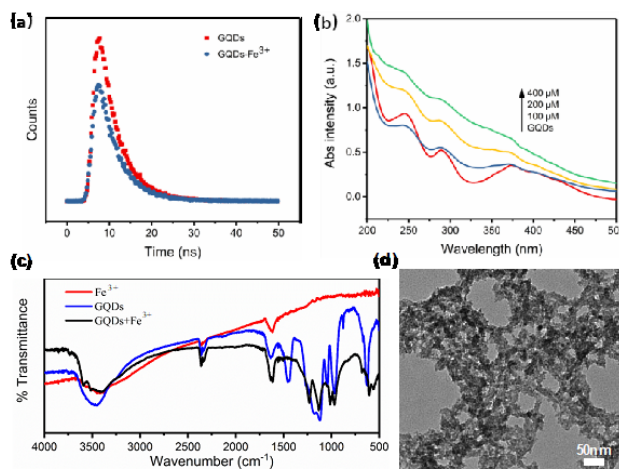


Figure 7. (a) Fluorescence decays (368 nm excitation) of sulfonic-GQDs by TCSPC in the presence (blue) and absence (red) of sulfonic-GQDs+ Fe^{3+} composite. (b) The UV-vis absorption intensity of sulfonic-GQD in the absence and presence of Fe^{3+} (100-400 μM). (c) FTIR spectra of GQDs and their composite. (d) TEM

image of the as-prepared sulfonic-GQDs + Fe³⁺ composite, Scale bar: 50 nm.

Table 2. The hydrate particle sizes of Fe³⁺, sulfonic-GQDs and sulfonic-GQDs+Fe³⁺ composite.

Samples	Hydrate particle size
Fe ³⁺	29.6±0.84
GQDs	—
GQDs-Fe ³⁺ composite	37.0±2.15

The standard Cell Counting Kit-8 (CCK-8) assays were performed to evaluate the cytotoxicity of sulfonic-GQDs in GES-1 cells (human normal gastric epithelial cell line). As shown in Figure 8, average cell viability of GES-1 cells was exceed 70% after 24 h culturing with sulfonic-GQDs at a concentration of 100 mg/L, while it was greater than 60% after 48 h. The similar results were detected in our previous paper, which showed amine- and OH-functionalized GQDs had no cytotoxicity at relatively high concentrations (The cell viabilities were >80% at 20, 40, 60 and 80 mg/L for 48h)[22].

It indicated that sulfonic-GQDs were minimally invasive/toxic to cells over 24 h and hence show promising biocompatibility. So, sulfonic-GQDs could be used to analyse food stuffs with further experiment and analysis.

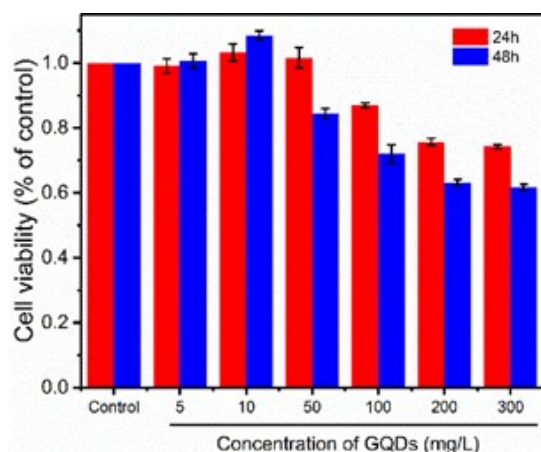


Figure 8. Cell viability of GES-1 cells incubated with various concentrations of sulfonic-GQDs.

4. CONCLUSIONS

In summary, we have developed a simple and practical way to detect Fe³⁺ ions based on effective FL probe sulfonic-GQDs with high sensitivity, selectivity and better biocompatibility. The FL intensity of sulfonic-GQDs versus the Fe³⁺ ions concentrations is a good linearity over a wide of detection concentration range from 5 to 100 μM, with a good detection limit of 407 nM. The results indicate that sulfonic-GQDs could meet the selective requirements for biomedical and environmental application and be sensitive enough to detect Fe³⁺ ions in environmental water samples. Moreover, according to the TCSPC and UV-vis absorbance analysis, we deduced that the quenching mechanism of the fluorescent probes for Fe³⁺ ions detection is static quenching rather than dynamic quenching. Furthermore, the low toxic, high chemical and photo stable sulfonic-GQDs fluorescent probe can be synthesised in mass production which shows a reality for the real application in the environment water sample analysis, food analysis and clinical diagnosis.

AUTHOR'S CONTRIBUTIONS

Y.L.W and M.H.W conceived and designed all the experiments. C.J.Y, X.J.X, W.C.G, L. D, P.D. performed all experiments. C.C.L&Y.N.H realized the material synthesis and characterization. C.J.Y&X.X.J co-wrote the paper. All authors discussed the results and analysed the data.

ACKNOWLEDGEMENTS

This work has been supported by the National Natural Science Foundation of China (Nos., 11575107, 21471097, 21571127, 21371115), Program for Changjiang Scholars and Innovative Research Team in University (No. IRT13078).

REFERENCES

1. F. Wang, Z. Gu, W. Lei, W. Wang, X. Xia, Q. Hao, Graphene quantum dots as a fluorescent sensing platform for highly efficient detection of copper(II) ions, *Sensors & Actuators: B. Chemical* 190(Complete) (2014) 516-522.
2. O. Sadak, A.K. Sundramoorthy, S. Gunasekaran, Highly selective colorimetric and electrochemical sensing of iron (III) using Nile red functionalized graphene film, *Biosensors and Bioelectronics* 89 (2017) 430-436. PMID:27132997 [View Article](#) [PubMed/NCBI](#)
3. L. Li, L. Li, C. Wang, K. Liu, R. Zhu, H. Qiang, Y. Lin, Synthesis of nitrogen-doped and amino acid-functionalized graphene quantum dots from glycine, and their application to the fluorometric determination of ferric ion, *Microchimica Acta* 182(3) (2015) 763-770. [View Article](#)
4. X. Liu, E.C. Theil, Ferritins: Dynamic Management of Biological Iron and Oxygen Chemistry, *Accounts of Chemical Research* 38(3) (2005) 167-175. PMID:15766235 [View Article](#) [PubMed/NCBI](#)
5. S.-P. Wu, Y.-P. Chen, Y.-M. Sung, Colorimetric detection of Fe³⁺ ions using pyrophosphate functionalized gold nanoparticles, *Analyst* 136(9) (2011) 1887-1891. PMID:21373691 [View Article](#) [PubMed/NCBI](#)
6. J.D. Haas, I.V.T. Brownlie, Iron Deficiency and Reduced Work Capacity: A Critical Review of the Research to Determine a Causal Relationship, *The Journal of Nutrition* 131(2) (2001) 676S-690S. PMID:11160598 [View Article](#) [PubMed/NCBI](#)
7. J.R. Burdo, J.R. Connor, Brain iron uptake and homeostatic mechanisms: An overview, *Biomaterials* 16(1) (2003) 63-75. PMID:12572665 [View Article](#) [PubMed/NCBI](#)
8. C.M.G. van den Berg, Chemical Speciation of Iron in Seawater by Cathodic Stripping Voltammetry with Dihydroxynaphthalene, *Anal. Chem.* 78(1) (2006) 156-163. + PMID:16383323 [View Article](#) [PubMed/NCBI](#)
9. Z.-Q. Liang, C.-X. Wang, J.-X. Yang, H.-W. Gao, Y.-P. Tian, X.-T. Tao, M.-H. Jiang, A highly selective colorimetric chemosensor for detecting the respective amounts of iron(ii) and iron(iii) ions in water, *New Journal of Chemistry* 31(6) (2007) 906-910. [View Article](#)
10. S. Lunvongsa, M. Oshima, S. Motomizu, Determination of total and dissolved amount of iron in water samples using catalytic spectrophotometric flow injection analysis, *Talanta* 68(3) (2006) 969-973. PMID:18970418 [View Article](#) [PubMed/NCBI](#)
11. D.M.C. Gomes, M.A. Segundo, J.L.F.C. Lima, A.O.S.S. Rangel, Spectrophotometric determination of iron and boron in soil extracts using a multi-syringe flow injection system, *Talanta* 66(3) (2005) 703-711. PMID:18970042 [View Article](#) [PubMed/NCBI](#)
12. J.E.T. Andersen, A novel method for the filterless pre-concentration of iron, *Analyst* 130(3) (2005) 385-390. PMID:15724169 [View Article](#) [PubMed/NCBI](#)
13. A. Matusch, C. Depboylu, C. Palm, B. Wu, G.U. Höglinger, M.K.H. Schäfer, J.S. Becker, Cerebral bi-oimaging of Cu, Fe, Zn, and Mn in the MPTP mouse model of Parkinson's disease using laser ablation inductively coupled plasma mass spectrometry (LA-ICP-MS), *Journal of the American Society for Mass Spectrometry* 21(1) (2010) 161-171. PMID:19892565 [View Article](#) [PubMed/NCBI](#)
14. J. Ju, W. Chen, Synthesis of highly fluorescent nitrogen-doped graphene quantum dots for sensitive, label-free detection of Fe (III) in aqueous media, *Biosensors and Bioelectronics* 58 (2014) 219-225. PMID:24650437 [View Article](#) [PubMed/NCBI](#)
15. R. Guo, S. Zhou, Y. Li, X. Li, L. Fan, N.H. Voelcker, Rhodamine-Functionalized Graphene Quantum Dots for Detection of Fe³⁺ in Cancer Stem Cells, *ACS Appl. Mater. Interfaces* 7(43) (2015) 23958-23966. PMID:26317667 [View Article](#) [PubMed/NCBI](#)
16. B. Kalyanaraman, V. Darley-Usmar, K.J.A. Davies, P.A. Dennery, H.J. Forman, M.B. Grisham, G.E. Mann, K. Moore, L.J. Roberts, H. Ischiropoulos, Measuring reactive oxygen and nitrogen species with fluorescent probes: challenges and limitations, *Free Radical Biology and Medicine* 52(1) (2012) 1-6. PMID:22027063 [View Article](#) [PubMed/NCBI](#)
17. F. Wang, L. Wang, X. Chen, J. Yoon, Recent progress in the development of fluorometric and colorimetric chemosensors for detection of cyanide ions, *Chem. Soc. Rev.* 43(13) (2014) 4312-4324. PMID:24668230 [View Article](#) [PubMed/NCBI](#)
18. H.-L. Zhang, Y. Zang, J. Xie, J. Li, G.-R. Chen, X.-P. He, H. Tian, A 'Clicked' Tetrameric Hydroxamic Acid Glycopeptidomimetic Antagonizes Sugar-Lectin Interactions On The Cellular Level, *Sci Rep* 4 (2014) 5513. PMID:24981800 [View Article](#) [PubMed/NCBI](#)
19. K.-B. Li, H. Wang, Y. Zang, X.-P. He, J. Li, G.-R. Chen, H. Tian, One-Step Click Engineering Considerably Ameliorates the Practicality of an Unqualified Rhodamine Probe, *ACS Appl. Mater. Interfaces* 6(22) (2014) 19600-19605. PMID:25379787 [View Article](#) [PubMed/NCBI](#)
20. H.Y.V. Ching, S. Clifford, M. Bhadbhade, R.J. Clarke, L.M. Rendina, Synthesis and Supramolecular Studies of Chiral Boronated Platinum(II) Complexes: Insights into the Molecular Recognition of Carboranes by β -Cyclodextrin, *Chemistry - A European Journal* 18(45) (2012) 14413-14425. PMID:23011948 [View Article](#) [PubMed/NCBI](#)
21. K.-B. Li, Y. Zang, H. Wang, J. Li, G.-R. Chen, T.D. James, X.-P. He, H. Tian, Hepatoma-selective imaging of heavy metal ions using a 'clicked' galactosylrhodamine probe, *Chem. Commun.* 50(79) (2014) 11735-11737. PMID:25144660 [View Article](#) [PubMed/NCBI](#)
22. L. Wang, Y. Wang, T. Xu, H. Liao, C. Yao, Y. Liu, Z. Li, Z. Chen, D. Pan, L. Sun, M. Wu, Gram-scale synthesis of single-crystalline graphene quantum dots with superior optical properties, *Nat. Commun.* 5 (2014) 5357. PMID:25348348 [View Article](#) [PubMed/NCBI](#)
23. D. Pan, J. Zhang, Z. Li, M. Wu, Hydrothermal Route for Cutting Graphene Sheets into Blue-Luminescent Graphene Quantum Dots, *Advanced materials* 22(6)

- (2010) 734-738. PMID:20217780 [View Article](#) [PubMed/NCBI](#)
24. L. Tang, R. Ji, X. Cao, J. Lin, H. Jiang, X. Li, K.S. Teng, C.M. Luk, S. Zeng, J. Hao, S.P. Lau, Deep Ultraviolet Photoluminescence of Water-Soluble Self-Passivated Graphene Quantum Dots, *ACS Nano* 6(6) (2012) 5102-5110. PMID:22559247 [View Article](#) [PubMed/NCBI](#)
 25. Z. Qian, J. Ma, X. Shan, L. Shao, J. Zhou, J. Chen, H. Feng, Surface functionalization of graphene quantum dots with small organic molecules from photoluminescence modulation to bioimaging applications: an experimental and theoretical investigation, *RSC Adv.* 3(34) (2013) 14571-14579. [View Article](#)
 26. H. Razmi, R. Mohammad-Rezaei, Graphene quantum dots as a new substrate for immobilization and direct electrochemistry of glucose oxidase: Application to sensitive glucose determination, *Biosensors and Bioelectronics* 41 (2013) 498-504. PMID:23098855 [View Article](#) [PubMed/NCBI](#)
 27. K. Habiba, V.I. Makarov, J. Avalos, M.J.F. Guinel, B.R. Weiner, G. Morell, Luminescent graphene quantum dots fabricated by pulsed laser synthesis, *Carbon* 64 (2013) 341-350. PMID:27570249 PMCid:PMC4999264 [View Article](#) [PubMed/NCBI](#)
 28. J. Shen, Y. Zhu, X. Yang, C. Li, Graphene quantum dots: emergent nanolights for bioimaging, sensors, catalysis and photovoltaic devices, *Chem. Commun.* 48 (31) (2012) 3686-3699. PMID:22410424 [View Article](#) [PubMed/NCBI](#)
 29. M. Xie, Y. Su, X. Lu, Y. Zhang, Z. Yang, Y. Zhang, Blue and green photoluminescence graphene quantum dots synthesized from carbon fibers, *Materials Letters* 93 (2013) 161-164. [View Article](#)
 30. L. Cao, M.J. Meziani, S. Sahu, Y.-P. Sun, Photoluminescence Properties of Graphene versus Other Carbon Nanomaterials, *Accounts of Chemical Research* 46(1) (2013) 171-180. PMID:23092181 [View Article](#) [PubMed/NCBI](#)
 31. J.M. Bai, L. Zhang, R.P. Liang, J.D. Qiu, Graphene Quantum Dots Combined with Europium Ions as Photoluminescent Probes for Phosphate Sensing, *Chemistry - A European Journal* 19(12) (2013) 3822-3826. PMID:23420738 [View Article](#) [PubMed/NCBI](#)
 32. L. Li, G. Wu, T. Hong, Z. Yin, D. Sun, E.S. Abdel-Halim, J.-J. Zhu, Graphene Quantum Dots as Fluorescence Probes for Turn-off Sensing of Melamine in the Presence of Hg²⁺, *ACS Appl. Mater. Interfaces* 6(4) (2014) 2858-2864. PMID:24460139 [View Article](#) [PubMed/NCBI](#)
 33. K. Zhang, J. Guo, J. Nie, B. Du, D. Xu, Ultrasensitive and selective detection of Cu²⁺ in aqueous solution with fluorescence enhanced CdSe quantum dots, *Sensors and Actuators B: Chemical* 190 (2014) 279-287. [View Article](#)
 34. Y. Dong, G. Li, N. Zhou, R. Wang, Y. Chi, G. Chen, Graphene Quantum Dot as a Green and Facile Sensor for Free Chlorine in Drinking Water, *Anal. Chem.* 84 (19) (2012) 8378-8382. PMID:22957474 [View Article](#) [PubMed/NCBI](#)
 35. J. Peng, W. Gao, B.K. Gupta, Z. Liu, R. Romero-Aburto, L. Ge, L. Song, L.B. Alemany, X. Zhan, G. Gao, S.A. Vithayathil, B.A. Kaiparettu, A.A. Marti, T. Hayashi, J.-J. Zhu, P.M. Ajayan, Graphene Quantum Dots Derived from Carbon Fibers, *Nano Lett.* 12(2) (2012) 844-849. PMID:22216895 [View Article](#) [PubMed/NCBI](#)
 36. S. Zhu, J. Zhang, C. Qiao, S. Tang, Y. Li, W. Yuan, B. Li, L. Tian, F. Liu, R. Hu, H. Gao, H. Wei, H. Zhang, H. Sun, B. Yang, Strongly green-photoluminescent graphene quantum dots for bioimaging applications, *Chem. Commun.* 47(24) (2011) 6858-6860. PMID:21584323 [View Article](#) [PubMed/NCBI](#)
 37. Z.M. Markovic, B.Z. Ristic, K.M. Arskin, D.G. Klisic, L.M. Harhaji-Trajkovic, B.M. Todorovic-Markovic, D.P. Kepic, T.K. Kravic-Stevovic, S.P. Jovanovic, M.M. Milenkovic, D.D. Milivojevic, V.Z. Bumbasirevic, M.D. Dramicanin, V.S. Trajkovic, Graphene quantum dots as autophagy-inducing photodynamic agents, *Biomaterials* 33(29) (2012) 7084-7092. PMID:22795854 [View Article](#) [PubMed/NCBI](#)
 38. S. Li, Y. Li, J. Cao, J. Zhu, L. Fan, X. Li, Sulfur-Doped Graphene Quantum Dots as a Novel Fluorescent Probe for Highly Selective and Sensitive Detection of Fe³⁺, *Anal. Chem.* 86(20) (2014) 10201-10207. PMID:25280346 [View Article](#) [PubMed/NCBI](#)
 39. A.P. Demchenko, The red-edge effects: 30 years of exploration, *Luminescence* 17(1) (2002) 19-42. PMID:11816059 [View Article](#) [PubMed/NCBI](#)
 40. B. Shi, Y. Su, L. Zhang, M. Huang, R. Liu, S. Zhao, Nitrogen and Phosphorus Co-Doped Carbon Nanodots as a Novel Fluorescent Probe for Highly Sensitive Detection of Fe³⁺ in Human Serum and Living Cells, *ACS Appl. Mater. Interfaces* 8(17) (2016) 10717-10725. PMID:27014959 [View Article](#) [PubMed/NCBI](#)
 41. S. Huang, H. Qiu, S. Lu, F. Zhu, Q. Xiao, Study on the molecular interaction of graphene quantum dots with human serum albumin: Combined spectroscopic and electrochemical approaches, *Journal of Hazardous Materials* 285 (2015) 18-26. PMID:25462867 [View Article](#) [PubMed/NCBI](#)